

A CONSTITUTIVE MODEL FOR FIBER REINFORCED POLYMER PLIES – COUPLING OF PLASTIC AND ELASTO–DAMAGE MECHANISMS

JAN H. KAUL, HEINZ E. PETTERMANN

Institute of Lightweight Design and Structural Biomechanics,
Vienna University of Technology
Getreidemarkt 9, A-1060 Vienna, Austria
kaul@ilsb.tuwien.ac.at - www.ilsb.tuwien.ac.at

Key words: Laminated composites, Anisotropic constitutive model, Damage mechanics, Plasticity, Implicit constitutive integration, Finite Element Analysis

Abstract. A constitutive model to predict the plastic and elasto-damage mechanisms of unidirectional fiber reinforced polymer plies is presented. The model predicts plastic strain accumulation and uses continuum damage mechanics to model the stiffness degradation accompanied by strain hardening behavior.

In this work an existing model is reformulated with focus on thermodynamic consistency, while maintaining the simple calibration procedure by commonly established experiments, particularly for the coupling of plasticity and damage. The internal damage and plasticity variables evolve according to mutually independent nominal and effective stress–strain curves, respectively. The constitutive rate equations are integrated numerically using an implicit scheme, which ensures that the consistency conditions are satisfied throughout the deformation process.

The anisotropic evolution of damage and plastic variables is calibrated to experimental data, obtained for transverse compressive and in–plane-shear loadings. The predictive capabilities of the proposed constitutive model are demonstrated on a single element under homogeneous combined compressive and in–plane shear strain loading conditions.

1 Introduction

Due to their high strength and stiffness to weight ratios, laminates made of unidirectional fiber reinforced polymer (FRP) plies are becoming increasingly popular in aeronautics and aerospace industries. To support their design process by numerical analysis tools, models for the mechanical response of such plies are required. Common models assume linear elastic behavior and assess the prevailing ply stresses by so-called first ply failure criteria. However, there are ply failure modes, that do not lead to immediate laminate failure and can be tolerated to some extent. Those modes are related primarily to the matrix material and correspond to its cracking and plastic yielding. To utilize the full

potential of FRP laminates, nonlinear ply constitutive models for such phenomena are desired to provide reliable predictions beyond the limits of linear elasticity.

In order to account for the gradually decreasing ply stiffness due to phenomena featuring brittle characteristics, models based on continuum damage mechanics have been developed [1, 2]. Most of them give reliable predictions, at least when the plies are loaded by transverse tensile stresses. However, in the presence of pronounced shear stresses in the ply, strains, that cannot be recovered after unloading, play an increasing role [3]. To incorporate this type of effects, constitutive models that combine continuum damage mechanics and plasticity theory have been developed [4, 5].

In the present work the hardening formulation of the constitutive ply model developed in [4, 5] is reformulated and extended. The extension aims at an concise mathematical formulation and a precise calibration for the anisotropic evolution of damage and plasticity by commonly established experiments.

2 Constitutive model

In order to predict the response of laminated composites, it is common to combine a constitutive law formulated at the ply level with lamination theory, which links overall deformations of the laminate to the individual ply strains. To achieve reliable predictions beyond the limits of linear elasticity, non-linear ply behavior has to be considered. The following considerations apply to plies made of unidirectional fiber reinforced polymers that are embedded in a laminate and with plane stress states. The material behavior of the pristine plies is taken to be transversely isotropic and linear elastic. Following the reasoning from the original constitutive model, proposed by [4, 5, 6], the non-linearities are caused mainly by stiffness degradation and accumulation of unrecoverable strains.

The stiffness degradation is attributed to matrix cracking, fiber matrix debonding and progressive fiber failure. The corresponding strains are modeled as being recoverable upon unloading. Thus, stiffness degradation is modeled by an elasto-damage model that consists of two parts. The first one deals with stiffness degradation due to distributed, matrix dominated phenomena and is accompanied by strain hardening behavior. The second one deals with stiffness degradation triggered by localized matrix dominated as well as fiber related phenomena and is accompanied by strain softening behavior. The original model introduces some damage variable d_1 to model fiber failure and some damage variables d_2 and d_3 to model matrix related damage. The present work proposes a reformulation of the hardening behavior for the matrix related phenomena and uses the formulations for fiber failure and the softening behavior from the original model.

The accumulation of unrecoverable strains is attributed to the formation of microscopic areas with inelastically deformed matrix material. The unrecoverable strains are referred to as plastic strains, since their evolution is described by a plasticity model. The reformulated plasticity model uses the hypothesis of total energy equivalence to express the plastic evolution equations in terms of effective variables, which can be determined from the damage formulation. The hypothesis of total energy equivalence postulates that the mechanical behavior of a damaged material in a damaged state can be derived from the equivalent material in a fictitious undamaged state, by replacing the state variables by

the corresponding effective state variables [7]. Therefore, the relation between the damage and the plasticity formulation is determined by the effective variables and no further assumptions have to be made.

To assure thermodynamic consistency, the constitutive model is formulated in the framework of thermodynamics of irreversible processes. Consequently, the irreversible damage and plastic yield process is described by a sequence of equilibrium states, which are characterized by a number of internal state variables.

2.1 Internal state variables

Internal damage variables. In the following the internal damage variables characterizing the stiffness degradation are introduced. The stiffness degradation is treated by the compliance tensor of the damaged material

$$\mathbb{C}(\mathbf{d}) = \left(\mathbb{I} + \frac{d_2}{1-d_2} \mathbb{D}_2 + \frac{d_3}{1-d_3} \mathbb{D}_3 \right) \mathbb{C}_0, \quad (1)$$

where \mathbb{C}_0 is the initial undamaged compliance tensor and \mathbb{I} the fourth order symmetric identity tensor. The damage variables d_2 and d_3 and their corresponding fourth order damage effect tensors \mathbb{D}_2 and \mathbb{D}_3 are introduced to model two distinct types of damage. The damage variable d_2 corresponds to the formation of microcracks, eventually leading to mode A and B fracture, predicted by the Puck fracture criterion [8], whereas the damage variable d_3 corresponds to the formation of microcracks leading to mode C fracture. In order to capture the anisotropic stiffness degradation, the damage effect tensors \mathbb{D}_2 and \mathbb{D}_3 are formulated by recourse to a micromechanics method, as described in [4]. Since the vector of damage variables $\mathbf{d} = (d_2 \ d_3)^T$ depends on the thermodynamic state, which also depends on the other internal state variables, they are given by their rate form,

$$\dot{\mathbf{d}} = \lambda_d \mathbf{D}, \quad (2)$$

and cannot be determined explicitly. The rate depends on the consistency parameter λ_d , to be defined. The vector

$$\mathbf{D} = \begin{pmatrix} 1 - \frac{\sin(\theta)}{\sin(\theta_{\max})} \\ \frac{\sin(\theta)}{\sin(\theta_{\max})} \end{pmatrix} \quad (3)$$

determines the ratio between the rates of d_2 and d_3 and depends on the fracture angle θ and the maximum fracture angle θ_{\max} , calculated by the Puck fracture criterion [8]. The definition of the internal damage variables naturally leads to the definition of the effective stress

$$\tilde{\boldsymbol{\sigma}} = \xi(\mathbf{d}) \boldsymbol{\sigma}, \quad (4)$$

with the stress tensor $\boldsymbol{\sigma}$ and the scalar function

$$\xi(\mathbf{d}) = \frac{1 - d_2 d_3}{(1 - d_2)(1 - d_3)}, \quad (5)$$

which follows from the micromechanics method, as given in [4].

Plastic strain. To model unrecoverable strains, the corresponding internal state variables and their flow rule are introduced. Assuming an additive decomposition of the total strain tensor

$$\boldsymbol{\varepsilon} = \boldsymbol{\varepsilon}^e + \boldsymbol{\varepsilon}^p \quad (6)$$

into elastic strain $\boldsymbol{\varepsilon}^e$ and plastic strain $\boldsymbol{\varepsilon}^p$, the plastic strain itself plays the role of an internal state variable. In this work, its evolution is defined in terms of effective variables, with the effective plastic strain defined as

$$\tilde{\boldsymbol{\varepsilon}}^p = \frac{1}{\xi(\mathbf{d})} \boldsymbol{\varepsilon}^p . \quad (7)$$

The corresponding rate equation

$$\dot{\boldsymbol{\varepsilon}}^p = \xi(\mathbf{d}) \lambda_p \frac{\partial f_p(\tilde{\boldsymbol{\sigma}}, \tilde{\mathbf{A}})}{\partial \tilde{\boldsymbol{\sigma}}} , \quad (8)$$

is given similar to an associated flow rule, where f_p is the yield condition in effective variables, $\tilde{\mathbf{A}}$ are the effective yield strengths and λ_p is the plastic consistency parameter, to be defined.

Internal hardening variables. In order to control the plastic evolution process the vector of internal hardening variables

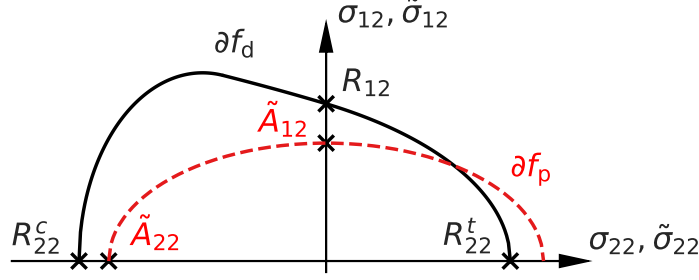
$$\tilde{\mathbf{a}} = \begin{pmatrix} \tilde{a}_{22} \\ \tilde{a}_{12} \end{pmatrix} \quad (9)$$

is introduced. The variable \tilde{a}_{22} can be interpreted as the equivalent effective plastic transverse normal strain and \tilde{a}_{12} as the equivalent effective plastic in-plane shear strain. They can evolve independent of each other and thus allow an anisotropic hardening behavior. The rate equation is given by

$$\dot{\tilde{\mathbf{a}}} = -\lambda_p \frac{\partial f_p(\tilde{\boldsymbol{\sigma}}, \tilde{\mathbf{A}})}{\partial \tilde{\mathbf{A}}} . \quad (10)$$

2.2 Initiation and evolution of damage and plasticity

The aim of the constitutive model is to establish a relation between stress rate and strain rate for any given material state. Every thermodynamic equilibrium state is defined by its internal state variables, which in turn are functions of the yet unknown consistency parameters λ_d and λ_p . In order calculate these, it is assumed that damage evolution and plastic yielding only takes place, when certain states, identified by the damage and yield conditions, are reached. The consistency parameters have to be chosen in a way that these states are maintained throughout the damage and/or yield process.


 Figure 1: Damage-onset surface ∂f_d and initial yield surface ∂f_p .

Damage and yield conditions. In order to identify the states in which damage evolution and accumulation of plastic strains occur, the damage and yield conditions are introduced. The damage condition f_d is formulated according to the Puck fracture criterion [8], which can be calculated in a closed form under plane stress assumptions. The corresponding damage surface

$$\partial f_d = \{(\boldsymbol{\sigma}, \mathbf{R}) \mid f_d(\boldsymbol{\sigma}, \mathbf{R}) = 0\} \quad (11)$$

is depicted in stress space in Figure 1. Instead of using the maximum strengths, the damage strengths $\mathbf{R} = (R_{22}^t, R_{22}^c, R_{12})^T$ are used to control the damage surface. The subscripts 22 and 12 denote the corresponding stress components, whereas the superscripts t and c denote either tensile or compressive loading. Initially the damage strengths take the values of damage-onset strengths and then evolve according to the hardening laws, to be defined. This way the damage surface ∂f_d may change its size and shape throughout the deformation process.

The yield condition

$$f_p(\tilde{\boldsymbol{\sigma}}, \tilde{\mathbf{A}}) = \frac{\tilde{\sigma}_{12}^2}{\tilde{A}_{12}^2} + \frac{\tilde{\sigma}_{22}^2}{\tilde{A}_{22}^2} - 1, \quad (12)$$

is defined in terms of the effective stress $\tilde{\boldsymbol{\sigma}}$ and the yield strengths $\tilde{\mathbf{A}} = (\tilde{A}_{22}, \tilde{A}_{12})^T$ and is assumed to be independent of the effective stress $\tilde{\sigma}_{11}$ in fiber direction. The effective yield strengths $\tilde{\mathbf{A}}$ are chosen to be the maximum effective normal stress under transverse compressive loading and the maximum effective shear stress under pure shear loading, before further plastic yielding occurs. This way the center of the corresponding yield surface

$$\partial f_p = \{(\tilde{\boldsymbol{\sigma}}, \tilde{\mathbf{A}}) \mid f_p(\tilde{\boldsymbol{\sigma}}, \tilde{\mathbf{A}}) = 0\} \quad (13)$$

is fixed, whereas the principal semi-axes change according to the yield strengths $\tilde{\mathbf{A}}$.

The damage and yield conditions are defined as non-positive functions, that have to be zero if damage evolution and plastic yielding respectively occurs. This can be expressed by the Kuhn-Tucker complementary conditions [9]

$$\lambda_d \geq 0, \quad f_d(\boldsymbol{\sigma}, \mathbf{R}) \leq 0, \quad \lambda_d f_d(\boldsymbol{\sigma}, \mathbf{R}) = 0, \quad (14)$$

$$\lambda_p \geq 0, \quad f_p(\tilde{\boldsymbol{\sigma}}, \tilde{\mathbf{A}}) \leq 0, \quad \lambda_p f_p(\tilde{\boldsymbol{\sigma}}, \tilde{\mathbf{A}}) = 0. \quad (15)$$

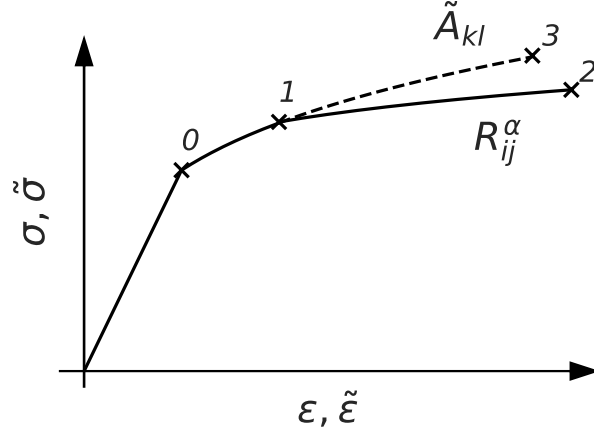


Figure 2: Sketch of the hardening laws, which are fitted to experimental data by supplying the values at the points 0 to 3.

The actual values of the consistency parameters can then be determined by the consistency conditions

$$\lambda_d \dot{f}_d(\boldsymbol{\sigma}, \mathbf{R}) = 0 \quad \text{if } f_d(\boldsymbol{\sigma}, \mathbf{R}) = 0 \quad (16)$$

$$\lambda_p \dot{f}_p(\tilde{\boldsymbol{\sigma}}, \tilde{\mathbf{A}}) = 0 \quad \text{if } f_p(\tilde{\boldsymbol{\sigma}}, \tilde{\mathbf{A}}) = 0 . \quad (17)$$

Hardening laws. To allow the damage and yield surfaces to evolve during loading, hardening laws for the damage strengths \mathbf{R} and effective yield strengths $\tilde{\mathbf{A}}$, in dependence of the internal state variables, are introduced. The hardening laws are defined in a way that they are able to reproduce the experimental data obtained from transverse tension, transverse compression and pure shear loadings. To achieve that, exponential laws of the form

$$R_{ij}^\alpha(\varepsilon_{ij}^{\text{el}}) = C_1 + C_2 \exp(-C_3 \varepsilon_{ij}^{\text{el}}) \quad \text{for } ij = \begin{cases} 22 \text{ and } \alpha = \text{c, t} \\ 12 \end{cases} \quad (18)$$

$$\tilde{A}_{kl}(\tilde{\varepsilon}_{kl}^{\text{p}}) = C_4 + C_5 \exp(-C_6 \tilde{\varepsilon}_{kl}^{\text{p}}) \quad \text{for } kl = 22, 12 , \quad (19)$$

are used for the hardening behavior. This enables to obtain stress–strain and effective stress–effective strain curves, like the ones depicted in Figure 2. The experimental data at the points 0 to 3 can be used to determine the constants C_1, C_2, C_4, C_5 , whereas the constants C_3, C_6 facilitate the shape fitting of the curves.

At this point the evolutions laws for the damage strengths \mathbf{R} depend on the strains measured in the experiments. In order to establish a relation to the internal damage variables, the compliance tensor from equation (1) can be used with equation (18) to obtain the expressions for $R_{22}^t(d_2, d_3), R_{22}^c(d_3), R_{12}(d_2, d_3)$, with direct dependence on the internal damage variables. The damage hardening law is formulated under the assumption, that the amount of damage fully characterizes the damage strength, independent of the actual stress state. Additionally, we assume that the damage variable d_2 , which is associated to

mode A and B fracture, doesn't influence the damage strength R_{22}^c . This is motivated by d_2 being related to cracks perpendicular to the transverse loading direction, which are assumed to have no effect on the integrity of the material under compressive loading.

2.3 Constitutive integration algorithm.

In order to use the constitutive model in a material subroutine for Finite Element computations, the stress, the internal state variables and the algorithmic consistent tangent stiffness have to be provided for a given strain increment. Since there is no closed form solution that solves the governing rate equations while satisfying the consistency conditions, a numerical integration scheme has to be used. In this work a semi-implicit integration scheme is used, that assures that the consistency conditions are satisfied for the obtained state. The algorithm calculates all variables implicitly, except for the fracture angle θ [8], which is used to define the ratio between the rates of the damage variables d_2 and d_3 . To reduce the computational complexity, the angle θ is calculated at the beginning of each increment and subsequently kept constant.

Because the stress tensor has to be provided as an output variable of the material subroutine and the damage and yield conditions depend on it, it is convenient to use it as a dependent variable for the solution process. Consequently, its rate equation is introduced before presenting the elastic predictor–inelastic corrector scheme, which is used to solve for the admissible state.

Stress rate. In order to establish the relation between the damage condition, the yield condition and the given strain rate, the relation between the stress rate and strain rate has to be known. Using the compliance tensor from equation (1) and the additive decomposition of the total strain, from equation (6), the stress rate is given by

$$\dot{\boldsymbol{\sigma}} = \mathbb{C}(\mathbf{d})^{-1} \left(\dot{\boldsymbol{\epsilon}} - \dot{\boldsymbol{\epsilon}}^p(\lambda_p) - \frac{d\mathbb{C}(\mathbf{d})\boldsymbol{\sigma}}{d\mathbf{d}} \dot{\mathbf{d}}(\lambda_d) \right). \quad (20)$$

At this point the stress rate depends on the internal state variables, whose relations to the strain rate are not given explicitly, but are expressed through the consistency parameters λ_d and λ_p . It is the objective of the algorithm presented in the next paragraph to compute these in a consistent way.

Elastic predictor – inelastic corrector scheme. A common approach for the integration of the constitutive rate equations is the predictor–corrector scheme. It uses an implicit solution scheme, where the initial guess is determined by an explicit step. The elastic predictor is driven by the strain increment and assumes the material state and hence the internal state variables to be constant. This way, a trial stress is calculated, which is used to evaluate the damage and yield condition. If either condition indicates inelastic behavior, the inelastic corrector is used to return the stress state to the damage and/or yield surface. According to the Kuhn-tucker complementary conditions, the scenarios of elastic unloading, pure plastic, pure damage and combined loading are possible.

In the following the focus is on the combined loading, since the other inelastic loadings can be obtained as special cases. In order to find an admissible state for a given strain increment, the rate equations for the stress and the internal state variables given in equations (20), (2), (8), (10) have to be integrated, while satisfying the consistency conditions. Implicit time integration to solve for an admissible the inelastic corrector step leads to the expression

$$\begin{pmatrix} \mathbb{C}\Delta\boldsymbol{\sigma} + \frac{d\mathbb{C}\boldsymbol{\sigma}^{n+1}}{d\mathbf{d}}\Delta\mathbf{d} + \xi(\mathbf{d})\Delta\lambda_p\frac{\partial f_p}{\partial\tilde{\boldsymbol{\sigma}}} \\ \Delta\mathbf{d} - \Delta\lambda_d\mathbf{D} \\ \Delta\tilde{\mathbf{a}} + \Delta\lambda_p\frac{\partial f_p}{\partial\tilde{\mathbf{A}}} \\ f_d(\boldsymbol{\sigma}^{n+1}, \mathbf{R}^{n+1}) \\ f_p(\tilde{\boldsymbol{\sigma}}^{n+1}, \tilde{\mathbf{A}}^{n+1}) \end{pmatrix} = 0, \quad (21)$$

where $\Delta\boldsymbol{\sigma}$, $\Delta\mathbf{d}$, $\Delta\tilde{\mathbf{a}}$ are the increments in the dependent variables, $\Delta\lambda_d$, $\Delta\lambda_p$ are the increments in the consistency parameters and n denotes the time increment of the numerical time integration scheme. Due to its complexity, the expression in equation (21) is iteratively solved by a Newton solver at the material subroutine level. The solution for the increments of the consistency parameters $\Delta\lambda_d$ and $\Delta\lambda_p$ are then used to update the internal state variables.

Algorithmic consistent tangent stiffness. In order to reach the desired convergence properties of the global Newton solver, the correct computation of the algorithmic consistent tangent stiffness, given by

$$\mathbb{J} = \begin{pmatrix} \mathbb{C}(\mathbf{d}) + (-\mathbb{I} & 0 & 0 & -\frac{d\mathbb{C}\boldsymbol{\sigma}}{d\mathbf{d}} & 0) \mathbb{L}^{-1} \begin{pmatrix} -\lambda_p\xi^2\frac{\partial^2 f_p(\tilde{\boldsymbol{\sigma}}, \tilde{\mathbf{A}})}{\partial\tilde{\boldsymbol{\sigma}}^2} \\ \lambda_p\xi\frac{\partial^2 f_p(\tilde{\boldsymbol{\sigma}}, \tilde{\mathbf{A}})}{\partial\tilde{\mathbf{A}}\partial\tilde{\boldsymbol{\sigma}}} \\ \xi\frac{\partial f_p(\tilde{\boldsymbol{\sigma}}, \tilde{\mathbf{A}})}{\partial\tilde{\boldsymbol{\sigma}}} \\ 0 \\ \frac{\partial f_d(\boldsymbol{\sigma}, \mathbf{R})}{\partial\boldsymbol{\sigma}} \end{pmatrix} \end{pmatrix}^{-1} \quad (22)$$

for the combined step, is important. It is computed at the end of each increment using the auxiliary matrix

$$\mathbb{L} = \begin{pmatrix} \mathbb{I} & -\xi\lambda_p\frac{\partial^2 f_p(\tilde{\boldsymbol{\sigma}}, \tilde{\mathbf{A}})}{\partial\tilde{\boldsymbol{\sigma}}\partial\tilde{\mathbf{A}}}\frac{\partial\tilde{\mathbf{A}}}{\partial\tilde{\mathbf{a}}} & -\xi\frac{\partial f_p(\tilde{\boldsymbol{\sigma}}, \tilde{\mathbf{A}})}{\partial\tilde{\boldsymbol{\sigma}}} & -\lambda_p\frac{d\xi}{d\mathbf{d}}\left(\xi\frac{\partial^2 f_p(\tilde{\boldsymbol{\sigma}}, \tilde{\mathbf{A}})}{\partial\tilde{\boldsymbol{\sigma}}^2}\boldsymbol{\sigma} + \frac{\partial f_p}{\partial\tilde{\boldsymbol{\sigma}}}\right) & 0 \\ 0 & \lambda_p\frac{\partial^2 f_p(\tilde{\boldsymbol{\sigma}}, \tilde{\mathbf{A}})}{\partial\tilde{\mathbf{A}}^2}\frac{\partial\tilde{\mathbf{A}}}{\partial\tilde{\mathbf{a}}} + \mathbf{I} & \frac{\partial f_p(\tilde{\boldsymbol{\sigma}}, \tilde{\mathbf{A}})}{\partial\tilde{\mathbf{A}}} & \lambda_p\frac{d\xi}{d\mathbf{d}}\frac{\partial^2 f_p(\tilde{\boldsymbol{\sigma}}, \tilde{\mathbf{A}})}{\partial\tilde{\mathbf{A}}\partial\tilde{\boldsymbol{\sigma}}}\boldsymbol{\sigma} & 0 \\ 0 & \frac{\partial f_p(\tilde{\boldsymbol{\sigma}}, \tilde{\mathbf{A}})}{\partial\tilde{\mathbf{A}}}\frac{\partial\tilde{\mathbf{A}}}{\partial\tilde{\mathbf{a}}} & 0 & \frac{d\xi}{d\mathbf{d}}\frac{\partial f_p(\tilde{\boldsymbol{\sigma}}, \tilde{\mathbf{A}})}{\partial\tilde{\boldsymbol{\sigma}}}\boldsymbol{\sigma} & 0 \\ 0 & 0 & 0 & \mathbf{I} & -\mathbf{D} \\ 0 & 0 & 0 & \frac{\partial f_d(\boldsymbol{\sigma}, \mathbf{R})}{\partial\mathbf{R}}\frac{d\mathbf{R}}{d\mathbf{d}} & 0 \end{pmatrix} \quad (23)$$

and the second order identity tensor \mathbf{I} .

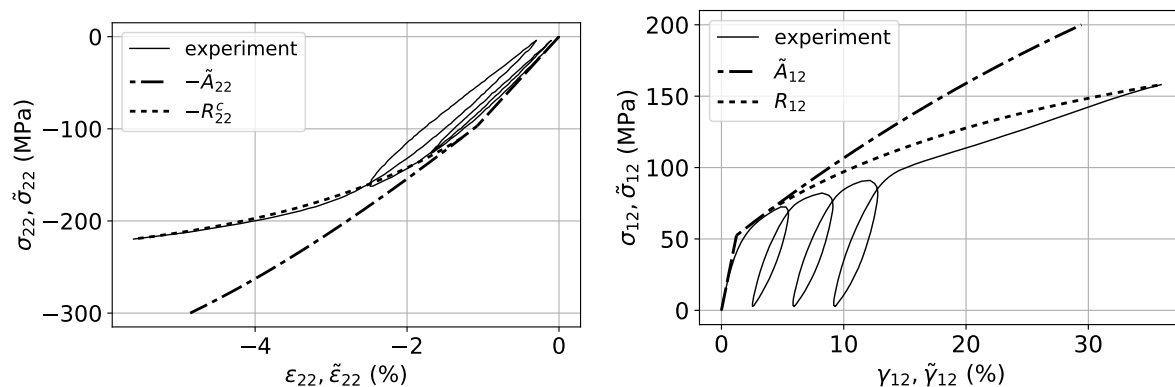


Figure 3: Experimental results [6] and hardening laws for transverse compression (left) and in-plane shear (right).

3 Application

The proposed model is implemented in a user subroutine UMAT for the Finite Element Software ABAQUS/Standard 2017 (SIMULIA, Providence, RI, USA). To assess the capabilities of the model, its prediction for the material system Cycom[®]977-2-35/40-12KHTS-134-300, in the following referred to as Cycom977, is studied for a single element simulation with homogeneous loading conditions.

3.1 Calibration of material data

The hardening laws from equations (18), (19) have to be calibrated by recourse to experimental data for transverse tensile, transverse compressive and pure shear loadings. In the context of this work only the compressive and shear loadings are considered. The calibration for the Cycom977 material is performed by stress-strain curves from [6] for a 0°-ply under transverse compression and a ±45°-laminate under tension [6], depicted in Figure 3. The tensile loading of the ±45°-laminate leads to a predominant shear stress in the ply principal axes and the obtained data can hence be used for the hardening law for shear loading.

In order to calibrate the plastic evolution, the hardening laws of the yield strengths $\tilde{\mathbf{A}}$ have to be determined. This is done by using the unloading curves to calculate the compliance and, consequently, the value of the damage variables at the according points. The damage variables provide a relation to determine the effective stress from the stress measured in the experiment. The resulting hardening laws are depicted in Figure 3.

3.2 Results

In the following, the results for a test case are presented. To induce damage evolution and plastic yielding simultaneously, a radial in-plane shear and compressive normal strain is applied. The initial damage and yield surfaces and the predicted stress path are shown in Figure 4. The ply behavior is linear elastic until it reaches the initial yield surface ∂f_p

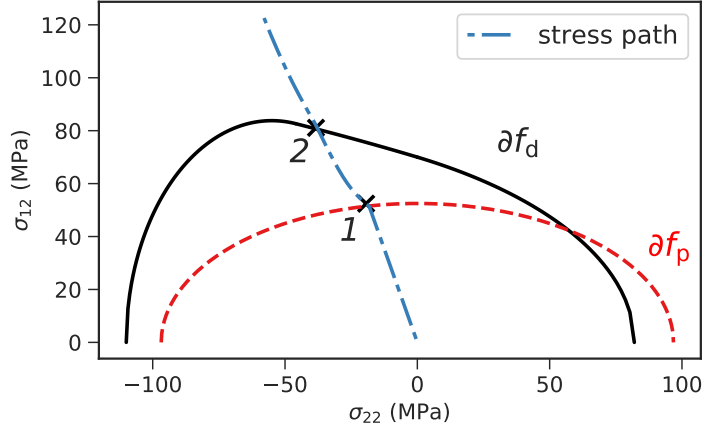


Figure 4: Initial damage surface ∂f_d , initial yield surface ∂f_p and stress path under combined compressive and in-plane shear loading.

at an applied strain of $\gamma_{12} = 0.014$ and $\varepsilon_{22} = -0.0023$ at point 1. The incipient plastic yielding leads to a kink in the stress path, resulting in a higher ratio of compressive stress to shear stress. The plastic yielding continues until it reaches the initial damage surface ∂f_d at an applied strain of $\gamma_{12} = 0.075$ and $\varepsilon_{22} = -0.0125$ at point 2. The subsequent evolution comprises plastic yielding as well as damage accumulation.

In the following, the damage model is examined in more detail. The evolution of the damage variables d_2 , d_3 , and the in-plane shear stress for the same load case is depicted in Figure 5. The response is linear elastic until the applied strain reaches the value of $\gamma_{12} = 0.014$ and $\varepsilon_{22} = -0.0023$. At 84 MPa, damage is initiated under mode B and the damage variable d_2 increases. Due to the fact, that the damage surface evolves according to the damage variables, also the boundary, distinguishing mode B and mode C, changes. In this case the loading leads to a change from mode B to mode C, where also the damage variable d_3 accumulates.

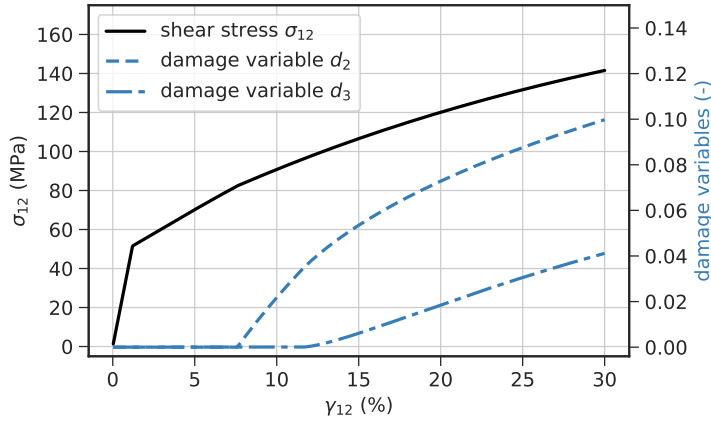


Figure 5: Shear stress and damage evolution under compressive, in-plane shear loading.

4 Conclusion

A constitutive model for plastic and elasto–damage mechanisms of fiber reinforced polymer plies is presented. It models the matrix dominated failure mechanisms and uses internal damage and plastic state variables to describe the stiffness degradation and accumulation of plastic strains. The governing constitutive rate equations are integrated using a semi-implicit integration scheme, while certain damage and yield conditions are satisfied. The anisotropic evolution of damage and plastic variables is calibrated to experimental data obtained for compressive and in–plane-shear loading.

The predictive capabilities of the proposed model are shown for a test case under homogeneous loading conditions. The result shows that the model is able to predict the simultaneous evolution of different damage variables and plastic strains.

REFERENCES

- [1] P. Maimí, P. P. Camanho, J. Mayugo, and C. Dávila, “A continuum damage model for composite laminates: Part i–constitutive model,” *Mechanics of Materials*, vol. 39, no. 10, pp. 897–908, 2007.
- [2] A. Matzenmiller, J. Lubliner, and R. Taylor, “A constitutive model for anisotropic damage in fiber-composites,” *Mechanics of materials*, vol. 20, no. 2, pp. 125–152, 1995.
- [3] W. Van Paepegem, I. De Baere, and J. Degrieck, “Modelling the nonlinear shear stress–strain response of glass fibre-reinforced composites. part i: Experimental results,” *Composites science and technology*, vol. 66, no. 10, pp. 1455–1464, 2006.
- [4] T. Flatscher and H. Pettermann, “A constitutive model for fiber-reinforced polymer plies accounting for plasticity and brittle damage including softening–implementation for implicit fem,” *Composite Structures*, vol. 93, no. 9, pp. 2241–2249, 2011.
- [5] T. Flatscher, C. Schuecker, and H. Pettermann, “A constitutive ply model for stiffness degradation and plastic strain accumulation: Its application to the third world wide failure exercise (part a),” *Journal of Composite Materials*, vol. 47, no. 20-21, pp. 2575–2593, 2013.
- [6] T. Flatscher, *A Constitutive Model for the Elasto-Plasto-Damage Ply Behavior in Laminated FRP Composites: Its Development, Implementation, and Application in FEM Simulations*. PhD thesis, Institut für Leichtbau und Struktur-Biomechanik, TU Wien, 2010.
- [7] K. Saanouni, C. Forster, and F. B. Hatira, “On the anelastic flow with damage,” *International Journal of Damage Mechanics*, vol. 3, no. 2, pp. 140–169, 1994.
- [8] M. Knops, *Analysis of failure in fiber polymer laminates: the theory of Alfred Puck*. Springer Science & Business Media, 2008.

- [9] D. G. Luenberger, Y. Ye, *et al.*, *Linear and nonlinear programming*, vol. 2. Springer, 1984.
- [10] J. Lemaitre, “A continuous damage mechanics model for ductile fracture,” *Journal of engineering materials and technology*, vol. 107, no. 1, pp. 83–89, 1985.